# *Candida antarctica* Lipase B Chemically Immobilized on Epoxy-Activated Micro- and Nanobeads: Catalysts for Polyester Synthesis

Bo Chen,[†] Jun Hu,[†] Elizabeth M. Miller,[‡] Wenchun Xie,[†] Minmin Cai,[†] and Richard A. Gross*,[†]

*NSF I/UCRC for Biocatalysis and Bioprocessing of Macromolecules, Polytechnic University, 6 Metrotech Center, Brooklyn, New York 11201, Rohm and Haas Company, P.O. Box 904, Spring House, Pennsylvania 19477*

*Received August 25, 2007; Revised Manuscript Received November 16, 2007*

*Candida antarctica* Lipase B (CALB) was covalently immobilized onto epoxy-activated macroporous poly(methyl methacrylate) Amberzyme beads (235 $\mu$m particle size, 220 Å pore size) and nanoparticles (nanoPSG, diameter 68 nm) with a poly(glycidyl methacrylate) outer region. Amberzyme beads allowed CALB loading up to 0.16 g of enzyme per gram of support. IR microspectroscopy generated images of Amberzyme−CALB beads showed CALB is localized within a 50 $\mu$m thick loading front. IR microspectroscopy images, recorded prior to and after treatment of Amberzyme−CALB with DMSO/aqueous Triton X-100, are similar, confirming that CALB is largely chemically linked to Amberzyme. The activity of CALB immobilized on Amberzyme, Lewatit (i.e., Novozym 435 catalyst), and nanoPSG was assessed for lactone ring-opening and step-condensation polymerizations. For example, the percent conversion of $\epsilon$-caprolactone using the same amount of enzyme catalyzed by Amberzym−CALB, Novozym 435, and nanoPSG−CALB for 20 min was 7.0, 16, and 65%, respectively. Differences in CALB reactivity were discussed based on resin physical parameters and availability of active sites determined by active site titrations. Regardless of the matrix used and chemical versus physical immobilization, $\epsilon$-CL ring-opening polymerizations occur by a chain growth mechanism without chain termination. To test Amberzyme−CALB stability, the catalyst was reused over three reaction cycles for $\epsilon$-CL ring-opening polymerization (70 °C, 70 min reactions) and glycerol/1,8-octanediol/adipic acid polycondensation reactions (90 °C, 64 h). Amberzyme−CALB was found to have far better stability for reuse relative to Novozym 435 for the polycondensation reaction.

## Introduction

*Candida antarctica* Lipase B (CALB) has proven to be a versatile catalyst for a wide range of biotransformations.[1–3] By attachment of enzymes onto solid supports, enhanced enzyme activity, selectivity, stability, and reusability in organic media may be achieved compared to the native enzyme.[4] Furthermore, macroporous resins, due to their large surface area, have been of greatest interest for CALB immobilization.[5] For these reasons, CALB was physically immobilized onto Lewatit VP OC 1600 (supplied by Bayer) that consists of poly(methyl methacrylate-*co*-divinylbenzene) and has average values of particle size, surface area, and pore diameter of 315–1000 $\mu$m, 130 $m^2\ g^{-1}$, and 150 Å, respectively (see product literature). This immobilized form of CALB, known as Novozym 435 and developed by Novozymes, is commercially available. Indeed, numerous publications document the utility of Novozym 435 as an extraordinary catalyst for both small organic molecules[6–10] and, more recently, for polymerization reactions.[11–17] However, recent studies in our laboratory show that Novozym 435 suffers from physical desorption or leaching of CALB during reactions (unpublished results). In some applications, such as for medical materials, protein contaminants in products may be unacceptable. Furthermore, processes that require multiple reuse cycles of Novozym 435 will be unattainable if substantial leaching of CALB occurs. This underscores the need to develop chemically immobilized CALB catalysts that overcome the above shortcomings of Novozym 435 while providing comparable activity for a wide range of biotransformations.

Some examples exist in the literature of covalently immobilized CALB catalysts. Palomo et al.[18] immobilized CALB on various activated carriers including octyl sepabeads, PEI−agarose, glyoxyl−agarose, glutaraldehyde−agarose, and Eupergit−Cu. By using CALB covalently immobilized onto the glutaraldehyde derivative, the (*S*)-ester and (*R*)-acid of (*RS*)-2-butyroyl-2-phenylacetic acid were obtained with high enantioselectivity ($E > 400$). In contrast, by interfacial adsorption of CALB onto octadecyl−Sepabeads, no appreciable enantioselectivity was achieved ($E = 2$ at pH 5). Also, CALB was covalently attached on dynamic membranes deposited with two water-soluble polymers (gelatin and/or polyethyleneimine, PEI) and activated glutaraldehyde on a ceramic $\alpha$-alumina support.[19] CALB dynamic membranes showed excellent operational stability in anhydrous media. The CALB−membrane derivative, prepared with gelatin−PEI, showed $28 \times 10^{-2}$ U $cm^{-}$ synthetic activity and a 203 day half-life in hexane media. Fernandez-Lorente et al.[20] first adsorbed CALB on an aminated silica gel and then cross-linked the adsorbed enzyme with glutaraldehyde in the presence of detergent. The activity of this immobilized CALB system for olive oil hydrolysis was 20 times lower relative to adsorbed CALB on polypropylene.

Epoxy-activated resins are generally considered ideal carriers for performing covalent immobilization of various proteins for

* Corresponding author. E-mail: rgross@poly.edu. Telephone 718-260-3024. Fax: 718-260-3075.
[†] NSF I/UCRC for Biocatalysis and Bioprocessing of Macromolecules, Polytechnic University.
[‡] Rohm and Haas Company.

10.1021/bm700949x CCC: $40.75 
Published on Web 01/16/2008

laboratory and industrial applications due to their compatibility with a wide range of enzymes.[21–24] The materials are easily stored and allow facile covalent bond attachment of proteins under mild conditions. For example, chemical coupling of penicillin G acylase to microporous epoxy-activated acrylic supports (Eupergit C) resulted in 100-fold enhanced enzyme stability relative to nonimmobilized soluble penicillin G acylase.[25] Huwig et al.[26] reported that immobilized pyranose oxidase from *Peniophora gigantea* on Eupergit C 250 showed only a 4% loss of activity during one 24 h operation cycle in which D-glucose is oxidized to 2-keto-D-glucose. Residual activity after six cycles was 76% compared to a 50% loss in activity for the free enzyme after one reaction cycle. Ivanov and Schneider[27] evaluated operational stability of the immobilized lipase from *Pseudomonas fluorescens* on several carriers including Eupergit C 250 L and glutaraldehyde activated silica. Fifty percent of the initial activity for immobilized Eupergit C 250 L was lost after three cycles of esterification for 1-phenylethanol and vinyl acetate in *t*-butylmethyl ether. In contrast, immobilized glutaraldehyde activated silica retained only around 12% of initial activity after three esterification cycles.

Despite interesting work exploring enzyme immobilization on epoxy-functionalized carriers, to the best of our knowledge, studies have not been performed to evaluate CALB immobilized on epoxy beads. Furthermore, previous work on enzyme immobilization on epoxy beads generally assumes all protein molecules are covalently attached and distributed throughout the immobilization matrix. Enzyme immobilization on epoxy-activated beads is believed to occur by the following two step mechanism: (i) enzyme adsorption onto the bead surface, and (ii) a covalent bond was formed.[28] Therefore, enzyme can be attached on supports by physical adsorption only. Moreover, studies of enzyme activities on epoxy-immobilized beads have been limited to small molecule biotransformations. Nevertheless, many enzymes immobilized on epoxy-functionalized supports have proven to be useful catalysts for low-molar-mass enzyme-catalyzed chemistries.

This paper reports systematic studies performed on CALB immobilized onto epoxy-activated macroporous poly(methyl methacrylate) Amberzyme beads (235 $\mu$m particle size, 220 Å pore size) and nanoparticles (diameter 68 nm). CALB loading was determined as a function of enzyme-to-resin ratio. Infrared (IR) microspectroscopy provided information on the distribution of immobilized CALB within Amberzyme beads. For comparison, nanoparticles, consisting of a polystyrene core and polyglycidyl methacrylate shell (nanoPSG), were prepared and used to immobilize CALB. Active site titration provided information on how CALB immobilization onto Amberzyme, Lewatit VP OC 1600 and nanoPSG altered the fraction of active CALB molecules. Effects of bead characteristics (e.g., particle and pore size) on polyester synthesis activities of Amberzyme−CALB, nanoPSG−CALB, and Novozym 435 were assessed. In addition, changes in Amberzyme−CALB and Novozym 435 activity during multiple polyester synthesis reaction cycles were determined. The results reported herein provide important insights into new CALB catalysts for polyester synthesis that consist of CALB chemically immobilized through epoxy ring-opening onto macroporous beads and nanoparticles.

## Experimental Section

**Materials.** *Candida antarctica* Lipase B (CALB) in the form of dried powder and Novozym 435 in which CALB is physically immobilized by the macroporous support, Lewatit VPOC 1600, were kind gifts from Novozymes (Bagsvaerd, Denmark). The SDS-PAGE analysis of an aqueous solution of this powder showed a single band with a molecular weight (33 KDa) corresponding to CALB. Amberzyme oxirane macroporous epoxy-activated poly(methyl methacrylate) resin with 235 $\mu$m average particle size, 220 Å average pore size, and 230 $m^2/g$ surface area was provided by Rohm and Haas Co. All chemicals were purchased from Sigma Chemical Co. in the highest available purity and were used without further purification.

**Determination of Epoxy Groups.** Resins activated by epoxy groups were dispersed in a solution consisting of 0.1 mol/L tetraethylammonium bromide in acetic acid. They were titrated with 0.1 mol/L perchloric acid solution until the crystal violet indicator changed to blue-green.

**Immobilization.** Amberzyme beads (0.1 g) were wetted by ethanol and then mixed into a 10 mL aqueous solution of CALB (1 mg/mL, 50 mM phosphate buffer, pH 7.8) at room temperature. Aliquots (250 $\mu$L) were withdrawn from this mixture to determine enzyme concentration by UV adsorption measurements as a function of time. Subsequently, resins were washed twice with 10 mL of buffer, and then they were dried (in vacuo, 24 h). The procedure of immobilization for nanoparticles is as same as Amberzyme beads. The % loading of CALB on supports was calculated as the weight fraction of enzyme in catalysts.

**Desorption.** At 37 °C, immobilized CALB on epoxy beads (Amberzyme−CALB, 50 mg) was incubated for 30 min in 3 mL of DMSO. Amberzyme−CALB was then separated by filtration and washed three times with 5 mL portions of DMSO. Then recovered Amberzyme−CALB was incubated for 30 min in 3 mL of 5% Triton X-100 solution at 37 °C and washed three times with 5 mL portions of 5% Triton X-100 solution. Enzyme desorbed from beads into DMSO and Triton X-100% was measured by a modified bicinchoninic acid (BCA) assay at 562 nm.[29] Standard curves were established in DMSO and 5% Triton X-100 solutions using a modified BSA assay to measure protein concentration. Absorption values as a function of BSA concentration in both DMSO and 5% Triton X-100 solutions were nearly linear.

**Imaging of Protein Distribution by Infrared Microscopy.** The method here is identical to that described elsewhere.[5] In summary, infrared microscopy was employed to determine CALB distribution within beads. Beads were embedded in paraffin wax, and blocks were sectioned at a thickness of 8 $\mu$m using a stainless steel blade. Sections were coated on $BaF_2$ disks and placed in a standard FTIR slide mount for data collection. Spectra were collected in the transmission mode from 4000 to 750 $cm^{-1}$ by a Spotlight FTIR spectrometer (Perkin-Elmer). The peak areas of *A* (1610–1670 $cm^{-1}$) and *B* (1700–1760 $cm^{-1}$) are proportional to amounts of CALB and PMMA, respectively. Enzyme concentration was calculated from the peak area corresponding to CALB divided by that corresponding to the resin.

**Enzyme-Catalyzed Ring-Opening Polymerization of $\epsilon$-Caprolactone.** The activities of immobilized CALB preparations were determined for $\epsilon$-caprolactone ($\epsilon$-CL) polymerizations. Reactions were monitored by in situ $^1H$ NMR experiments with the NMR probe at 70 °C. $^1H$ NMR measurements were performed on a Bruker DPX 300 spectrometer. Chemical shifts were referenced to tetramethylsilane (TMS) at 0.00 ppm. Into 5 mm NMR tubes was transferred $\epsilon$-CL (0.06 mL) and toluene-$d_8$ (0.7 mL), and tubes were placed in an external bath set at 70 °C. Then immobilized resins were added. The weight ratio of CALB to $\epsilon$-CL was maintained at 1:100 for all ring-opening polymerization experiments. After every scan (around 5–8 min), NMR tubes were removed from the probe, shaken well to mix tube contents, and then inserted back in the probe for the next scan. This procedure was performed as rapidly as possible to avoid fluctuations in the reaction temperature.

For recycling studies, the solution was carefully separated from the catalyst using a syringe needle. Then enzyme beads within the NMR tube were washed with THF three times and toluene-$d_8$ once. Monomer ($\epsilon$-CL, 0.06 mL) and toluene-$d_8$ (0.7 mL) were transferred to the 5 mm NMR tube with recycled catalyst, and the polymerization and

monitoring of reactions was performed as above. The immobilized CALB was assessed for a total of three reaction cycles.

**Enzyme-Catalyzed Bulk Condensation of Glycerol, 1,8-Octanediol, and Adipic Acid.** Glycerol (0.248 g, 0.1 equiv), 1,8-octanediol (1.58 g, 0.4 equiv), and adipic acid (1.97 g, 0.5 equiv) were transferred into a 100 mL round-bottom flask. The contents of the flask were heated at 115 °C to obtain a monophasic solution of the monomer mixture. The reaction temperature was lowered to 90 °C, and Amberzyme−CALB or Novozym 435 (1% by wt CALB relative to the total weight of monomers) was added. The flask was sealed with a rubber septum, and the reaction was maintained at 90 °C with stirring. After the first 2 h of the reaction the reaction contents were maintained under reduced pressure (40 mmHg). The polymerization was terminated by dissolving the reaction mixture in excess THF at 64 and 24 h for the reaction catalyzed by Amberzyme−CALB and Novozym 435, respectively. The immobilized CALB was collected by filtration for the next cycle of condensation. After evaporating the solvent, the resulting product was then precipitated by slow addition to methanol. The final product was characterized by GPC. For the second and third cycles of condensation reactions, temperature and time, the amount of monomers, and the method of product and enzyme processing were identical to that described above for cycle 1.

**Active-Site Titration of Immobilized Lipase in Hexane.** The method for synthesis of inhibitor methyl *p*-nitrophenyl *n*-hexylphosphate (MNPHP) and active site titration was reported elsewhere.[5] In summary, a stock solution of methyl *p*-nitrophenyl *n*-hexylphosphate (MNPHP) was prepared by adding MNPHP (12.04 mg, 40 mmol) to 4 mL of dry diethyl ether. The MNPHP diethyl ether solution (40 $\mu$L) was added to dry hexane (1.96 mL). Immobilized enzyme was pre-equilibrated in desiccators with saturated KCL solution to the desired water activity ($a_w = 0.75$) at room temperature overnight. In a sealed vial, 2 mL of MNPHP diethyl ether/hexane solution ($a_w = 0.75$) was added to immobilized enzyme (50 mg). After a 16 h reaction at 25 °C with shaking, the solvent was removed by vacuum. The mixture was then washed twice with 2 mL of acetonitrile (AcCN), and the concentration of *p*-nitrophenol was determined by LC-MS (see ref 5 for further details on LC-MS procedure). Afterward, carriers were washed with AcCN, dried by vacuum, and assayed for enzyme activity via ring-opening polymerization of $\epsilon$-CL for 30 min (see above).

**Synthesis, Characterization, and Immobilization of Nanoparticles.** The method of nanoparticle synthesis and purification was adapted from that described previously.[30,31] In a 1000 mL three-neck round-bottom flask equipped with stirrer, vacuum, and nitrogen inlet, a mixture of 10 g of freshly distilled styrene, 0.35 g of sodium dodecylsulphate, 0.1 g of divinylbenzene, and 0.34 g of sodium tetraborate in 105 g of water was stirred for 20 min at 400 rpm under nitrogen. The temperature was raised to 60 °C, and the starter (0.068 g of potassium peroxodisulphate in 17.5 mL of water) was added. The mixture was stirred and kept at constant temperature for 16 h. Then, 3 g of glycidyl methacrylate in 17.5 mL of methanol was added and the reaction was continued for 8 h at 60 °C. After completing the reaction, the latex was allowed to cool to room temperature and dialyzed for 30 min three times against distilled water. Monomer conversion, determined gravimetrically, was about 95%. The epoxy content, determined by titration with nascent hydrogen bromide in perchloric acid/butyrolactone[30] is 1.0 mmol/g. The nanoparticle size was 67.5 ± 1.4 nm, measured by static light scattering. The procedure for CALB immobilization is identical to that described above for epoxy-functionalized macroporous microparticles.

## Results and Discussion

Amberzyme was selected as a representative epoxy-activated macroporous resin for chemical immobilization of *Candida antartica* Lipase B (CALB). The chemical composition of Amberzyme is similar to Lewatit VPOC 1600. Lewatit VPOC 1600 macroporous beads have relatively larger average particle size than Amberzyme beads (315–1000 vs 235 $\mu$m). Its average values of surface area and pore size (130 $m^2\ g^{-1}$ and 150 Å, respectively) are smaller than that of Amberzyme (see above). For comparison, nanoparticles consisting of a polystyrene core and polyglycidyl methacrylate shell (nanoPSG) were prepared and used to immobilize CALB (see Experimental Section). Similar to Amberzyme beads, nanoPSG has activated epoxy groups for chemical immobilization of CALB. However, nanoPSG particles are much smaller (68 nm) and are nonporous. Interest in exploring nanoparticles as carriers for CALB was stimulated by an earlier study in our laboratory, where it was discovered that, by decreasing the particle size of PMMA macoporous supports from 560 to 710 to 35 $\mu$m, large increases in physically immobilized CALB activity were obtained.[5]

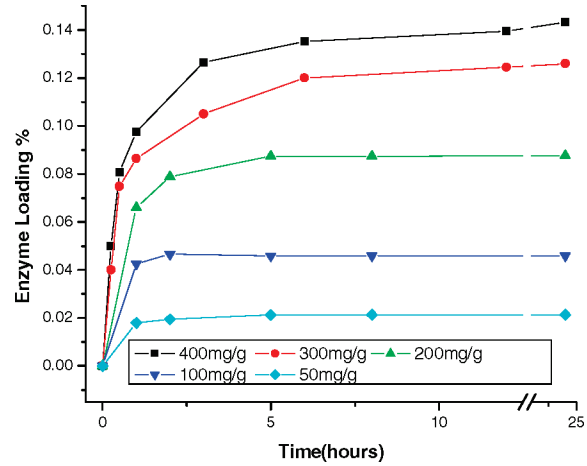


**Figure 1.** Results of CALB chemical immobilization on epoxy-activated Amberzyme resin using different enzyme/resin weight ratios.

**Enzyme Loading.** Maximum loading of CALB on Amberzyme resin, assuming each protein molecule is linked by one epoxy functional group and all epoxides are consumed, can reach 66 g per gram of support (0.29 $g \cdot m^{-2}$). By virtue of this high functional group density, a large fraction of immobilized protein should be chemically linked to the support. In other words, the high density of epoxy functional groups on Amberzyme beads should minimize the fraction of physically adsorbed CALB.[32]

Figure 1 shows adsorption isotherms of CALB on Amberzyme resin using CALB solutions that differ in concentration. For each concentration studied, loading saturation was achieved in ≤5 h. A previous study by our laboratory showed that loading saturation, performed by a similar immobilization protocol, gave loading saturation in ~5 h for 120 $\mu$m diameter Amberchrom PMMA beads.[5] CALB loading on Amberzyme increased by increasing CALB concentration. At the highest ratio (w/w) of CALB to Amberzyme (400 mg CALB per g of resin) investigated, enzyme loading reached 14 wt % (0.61 $mg/m^2$) while the absorption yield was low (34%). Surprisingly, the absorption yield was relatively insensitive to protein concentration in the range of 100−400 mg CALB per g of resin. Indeed, at 100 mg CALB per g of resin, enzyme loading reached 4.0% and the absorption yield was 42%. The enzyme loading of nanoPSG is around 3.8% when using 200 mg CALB per g of the support. The immobilization yield is slightly lower than that with Amberzyme resins.

**Imaging of CALB Distribution in Amberzyme Beads by IR Microspectroscopy.** Figure 2A displays the distribution of CALB on Amberzyme resin prepared by using a weight ratio of CALB to resin of 200 mg/g and loading time of 48 h. The

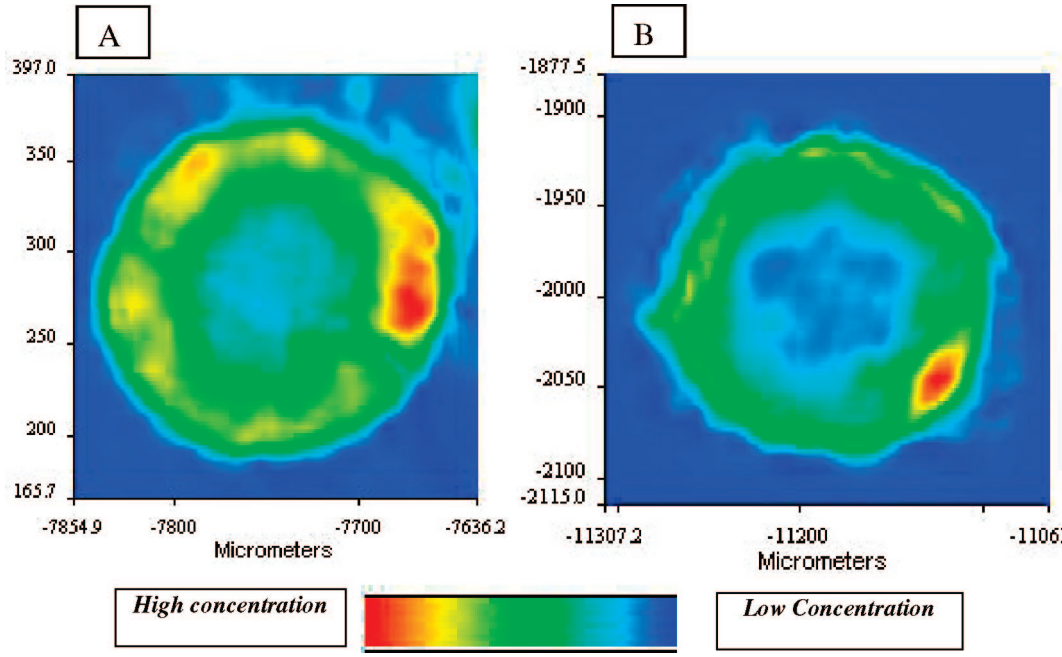


**Figure 2.** Distribution of CALB on Amberzyme resin as determined by IR microspectroscopy: (A) displays the image for Amberzyme−CALB prior to treatment with DMSO and Triton X-100, (B) displays the image for Amberzyme−CALB after extraction with DMSO and Triton X-100.

resulting Amberzyme−CALB catalyst system had CALB loading of 7.3%. Inspecting the IR image in Figure 2A shows that CALB is localized within a loading front of 50 $\mu$m thickness. Similarly, CALB immobilization on ~600 $\mu$m diameter Lewatit VPOC 1600 to prepare Novozym 435 resulted in a 80–100 $\mu$m thick loading front. Adsorbed CALB on Amberchrom PMMA resins with particle sizes 560–710 and 120 $\mu$m showed protein loading fronts with thicknesses of 100 and 40 $\mu$m, respectively.[5] Nonuniformity of image densities demonstrates CALB is unequally distributed throughout the loading front. Formation of a loading front with nonuniform image density is explained by restricted diffusion of CALB within pores.[33] This effect is amplified when the characteristic size of the enzyme is similar to the pore size of the support. Bosley and co-workers[29] found that unrestricted access of protein into the matrix can be achieved when the pore diameter is approximately 4−5 times the size of the enzyme. A recent study by our laboratory using flat surfaces has shown that CALB tends to adsorb onto surfaces as single molecules, not as dimmers or higher aggregates (manuscript in preparation). However, it is still possible that physical barriers prevent CALB's diffusion into the beads' core due to a nonhomogeneous distribution of pore sizes. Indeed, the dimensions of CALB based on its crystal structure is 30 Å × 40 Å × 50 Å,[34] while the average pore size within Amberzyme beads is 220 Å. Another contributing factor may be repulsive interactions between immobilized and soluble CALB within resin pores that limits the access of soluble CALB molecules to internal bead regions.[35] Previous work by our laboratory showed that, by manipulating matrix−protein interactions by alteration in matrix chemistry, changes in loading front thickness resulted.[5] For example, CALB is able to diffuse further into internal bead regions to occupy surfaces for resins consisting of PMMA relative to polystyrene.

Determination of CALB adsorption onto Amberzyme resin does not provide information on the relative fractions of CALB that is chemically linked versus physically adsorbed. For example, Malmsten and Larsson[36] showed that, when trypsin was immobilized onto glycidyl methacrylate beads, only 50% of the protein was chemically linked. To determine the fraction of physically adsorbed CALB on Amberzyme resin, Amberzyme−CALB was treated by DMSO, followed by Triton X-100 5% solution (see Experimental Section). This method allowed quantitative extraction of physically adsorbed CALB from Novozym 435, which has a similar surface chemistry to Amberzyme resin (see above). CALB extraction from Novozym 435 using DMSO/Triton X-100 was confirmed by IR microspectroscopy, which gave visual evidence that CALB was no longer present within the immobilization support (i.e., Lewatit VPOC 1600 beads).[35]

To visually assess whether CALB can be extracted from Amberzyme−CALB, the extraction described above using DMSO and Triton X-100 5% solutions was performed on Amberzym−CALB. The image in Figure 2B was then recorded and compared with that in Figure 2A. These two images show similar loading fronts (~50 $\mu$m thickness) and CALB distribution patterns. Thus, unlike extraction of CALB from Novozym 435, where virtually all CALB was removed from Lewatit VPOC 1600, the similarity of images in parts A and B of Figure 2 suggests a large fraction of CALB remains within Amberzyme−CALB, presumably due to the fact that CALB is predominantly chemically linked and not physically adsorbed to this support.

**Assessing the Extent that CALB is Chemically Immobilized on Amberzyme Beads.** Because results from IR microspectroscopy are nonquantitative, the amount of CALB extracted in DMSO and Triton X-100 5% was determined by a modified bicinchoninic acid (BCA) assay (see Experimental Section). If the two-step mechanism of immobilization on epoxy-activated resins is correct, then the fraction of chemically bound enzyme will vary with enzyme loading time. Hence, for enzyme loading conditions with 200 mg CALB per g of resin, immobilization times of 12, 24, 48, and 72 h were studied. Consistent with Figure 1, total enzyme loading varied little for these incubation times (6.5, 6.8, 7.3, and 7.6%, respectively). Extraction and measuring protein content showed that % CALB leached for immobilization times of 12, 24, 48, and 72 h was 29, 21, 13, and 13%, respectively. Thus, the majority of CALB is covalently linked to resins by 12 h. With increase in incubation time from 12 to 24 and 48 h, small but significant increases in the fraction of covalently immobilized CALB were

observed. However, increase in the incubation time beyond 48 h had no significant effect on the fraction of covalently bound CALB. These results are consistent with the proposed two-step mechanism for enzyme immobilization on epoxy-activated beads discussed above.

**Immobilized CALB Activity for ϵ-CL Ring-Opening Polymerizations.** The activity of CALB immobilized on Amberzyme, Lewatit VPOC 1600 (i.e., Novozym 435 catalyst), and nanoPSG was assessed by ϵ-CL ring-opening polymerizations. Loadings of CALB on Amberzyme and Lewatit are similar (7.6 and 8.5% by wt, respectively), while loading on nanoPSG nanoparticles was lower (3.8%). The ratio of catalyst to monomer was adjusted so that, for all CALB−resin systems, the monomer to CALB ratio was 100:1 w/w. As shown previously,[5] different chemical shifts are observed for methylene protons (−OC$H_2$−) of ϵ-CL monomer, PCL internal repeat units, and chain terminal −C$H_2$−OH moieties. Hence, by in situ NMR monitoring, monomer conversion and polymer number-average molecular weight ($M_n$) were determined.

As illustrated in Figure 3A, the polymerization rate strongly depends on the matrix used for CALB immobilization. For example, at about 20 min reaction time, the turnover frequency (TOF) for ϵ-CL increased from 4.4 to 10.5 and 39.2 $s^{-1}$ for Amberzym−CALB, Novozym 435, and nanoPSG−CALB, respectively. Each experiment was repeated at least three times, and variability was assessed by comparison of apparent rate constant values, ($k_{app}$, $min^{-1}$, see below). Variability in $k_{app}$ values was ±5.1%, which validated the significance of data reported herein. Error bars were not included for conversion values in Figure 3 because, by using in situ NMR to determine % ϵ-CL conversion, times at which conversion values were measured between experimental runs varied slightly.

Plots of $\log([M]_0/[M]_t)$ versus time were constructed and are displayed in Figure 3B. All plots in Figure 3B demonstrate a linear relationship with correlation coefficients >0.99. Thus, regardless of the matrix used and chemical versus physical immobilization, monomer conversion followed a first-order rate law and termination reactions did not occur. Similar behavior was observed for ϵ-CL ring-opening polymerizations catalyzed by CALB immobilized on Lewatit VPOC 1600 and a series of polymethyl methacrylate and polystyrene resins.[5,37–39] The activity of CALB−catalysts immobilized on these supports was quantified by determining reaction kinetic constants ($k_{app}$) by taking slopes of $\log([M_o]/[M])$ versus time plots. For CALB immobilized on Amberzyme, Lewatit VPOC 1600, and nanoPSG, $k_{app}$ is 0.0026, 0.0049, and 0.0252, respectively. Thus, $k_{app}$ is less for CALB immobilized on Amberzyme than on Lewatit VPOC 1600. Interestingly, $k_{app}$ was 5 and 10 times greater using nanoPSG as opposed to Lewatit VPOC 1600 and Amberzyme as matrices for CALB immobilization, respectively. This higher activity of nanoPSG−CALB may be due to higher activation of the protein by more favorable surface−CALB interactions. Indeed, the surface of nanoPSG is polyglycidyl methacrylate, which is very different than that of Lewatit VPOC 1600 and Amberzyme. Enzyme conformation may be better maintained on nanoparticles than PMMA microparticles. Vertegel and Dordick[40] reported that, relative to larger nanoparticles, adsorption of lysozyme onto small nanoparticles resulted in less loss of lysozyme α-helicity and higher catalytic activity. Moreover, nanoPSG particles are nonporous and, therefore, all protein is restricted to particle surfaces. Hence, diffusion constraints due to restricted substrate diffusion through pores, encountered for Lewatit VPOC 1600 and Amberzyme−CALB catalysts, are not a factor for nanoPSG−CALB.

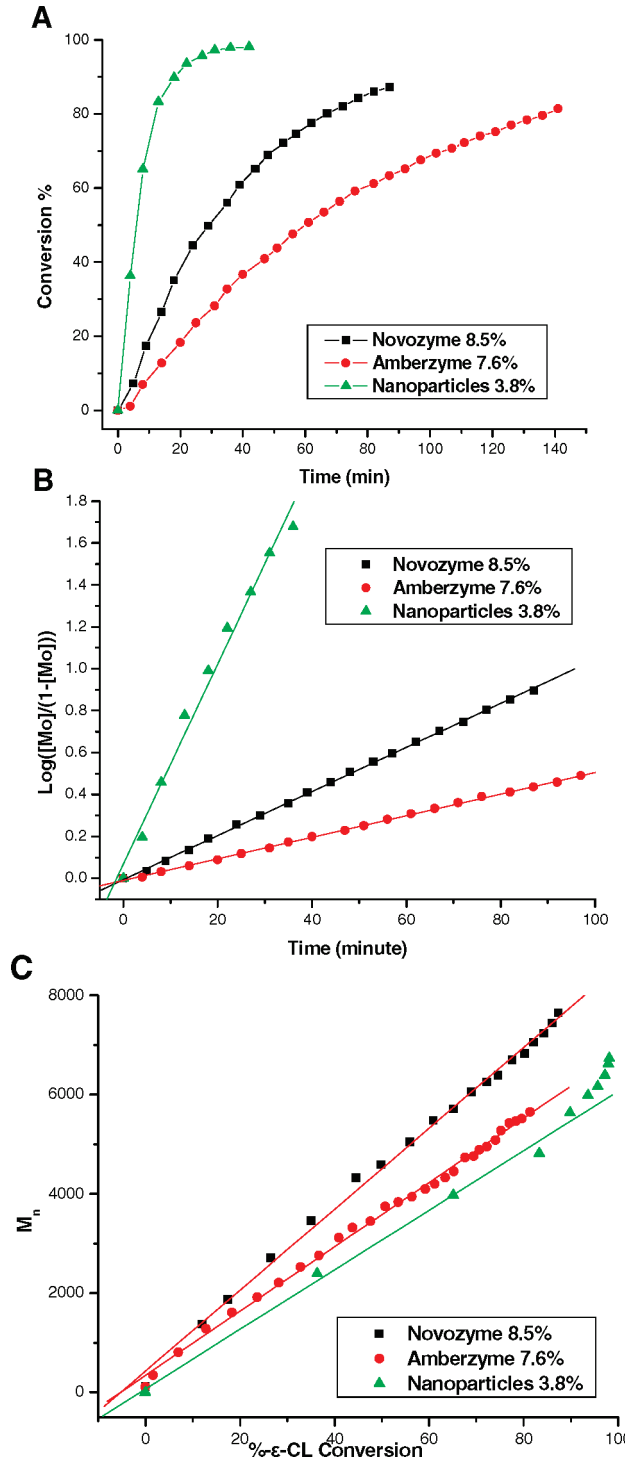


**Figure 3.** Immobilized CALB catalysis of ϵ-caprolactone ring-opening polymerizations performed at 70 °C in toluene-$d_8$ monitored by $^1$H NMR: (a) monomer conversion vs reaction time, (b) semilogarithmic plot, (c) $M_n$ vs % monomer conversion.

Explanations for higher ϵ-CL ring-opening polymerization activity of Novozym 435 relative to Amberzyme−CALB are discussed below. First, from titration experiments with *p*-nitrophenyl *n*-hexylphosphate (MNPHP) in hexane of Amberzyme−CALB and Novozym 435, % free active sites was 19.4 and 50.3, respectively. Hence, the higher fraction of active sites for immobilized CALB on Lewatit relative to Amberzyme is consistent with higher Novozym 435 activity. Lower active site availability for Amberzyme−CALB may result from covalent immobilization of CALB that restricts enzyme mobility

and reorientation after adsorption. Also, differences in surface chemistry due to epoxy functionalities may be responsible for orienting CALB in such a way that restricts access of substrates to immobilized CALB active sites.

Previous work by us and others used curve fitting of IR spectra in the amide I band region (1600–1700 $cm^{-1}$) to determine peak frequencies and intensities of amide I bands. This information enables estimation of α-helix and β-sheet content within proteins.[41,42] Details of this analysis for CALB immobilized on lewatit VPOC 1600 were published previously by our laboratory.[35] Indeed, by this method, CALB immobilized on Lewatit VPOC 1600 and free CALB both contained ~31% α-helix and ~19% β-sheet, which agrees with published X-ray crystallographic data.[34,35] Comparison of IR spectra for CALB immobilized on Lewatit VPOC 1600 and Amberzyme showed they were identical. Thus, CALB immobilized within these two supports shows no change in confirmation to the extent that can be detected by IR analysis. Nevertheless, results of CALB immobilization by covalent attachment to Amberzyme beads are promising because many parameters of these beads have yet to be optimized. For example, previous work by our laboratory showed that, by reducing the particle size of PMMA-based resins from 560 to 710, 120, 75, and 35 μm, the turnover frequency (TOF) for ϵ-CL polymerizations (80 min) increased from 3.0 to 4.9, 5.6, and 8.5 $s^{-1}$, respectively.[5] Furthermore, by using polystyrene-based macroporous beads for CALB physical immobilization, we found that, by increasing the pore size from 300 to 1000 Å, the TOF for 30 min ϵ-CL polymerizations increased from 12 to 28.2 $s^{-1}$. Also, by adjustment of surface features such as hydrophobic−hydrophilic balance and charge, further improvements in CALB activity and stability on epoxy-functionalized resins are expected. Finally, as will be discussed below, covalent immobilization is critical as a way to decrease enzyme leaching into product and thereby promote catalyst recyclability.

**Effects of Immobilization Support on Mechanism of CALB-Catalyzed ϵ-CL Ring-Opening Polymerizations.** Plots of $M_n$ versus % ϵ-CL conversion were constructed and are displayed in Figure 3C. All plots in Figure 3C demonstrate a linear relationship with correlation coefficients >0.99. Thus, regardless of the matrix used and chemical versus physical immobilization, polymerizations occur by a chain growth mechanism without chain transfer to monomer. Similar behavior was observed for ϵ-CL ring-opening polymerizations catalyzed by CALB immobilized on Lewatit VPOC 1600,[39] commercial resins studied by Nakaoki et al.,[43] a series of polymethyl methacrylate[5] and polystyrene resins.[44] Because water content in reactions is similar, the total number of propagating PCL chains should also be similar for CALB immobilized on Lewatit VPOC 1600, Amberzyme, and nanoPSG. Hence, this explains why $M_n$ at fixed monomer conversion values changed little as a function of the resin used.

**Effects of CALB Loading on Amberzyme−CALB Activity for CALB-Catalyzed ϵ-CL Ring-Opening Polymerizations.** Extraction experiments described above showed % CALB leached for immobilization times of 12, 24, 48, and 72 h was 29, 21, 13, and 13%, respectively. Hence, small but significant increases in the fraction of covalently immobilized CALB were observed by extending the immobilization time. The possibility that these changes in the fraction of chemically immobilized CALB would affect catalyst activity was studied. Plots in Figure 4 are overlapped, showing that changes in the immobilization time from 12 to 72 h and corresponding changes in the fraction of chemically immobilized CALB had no significant effect on

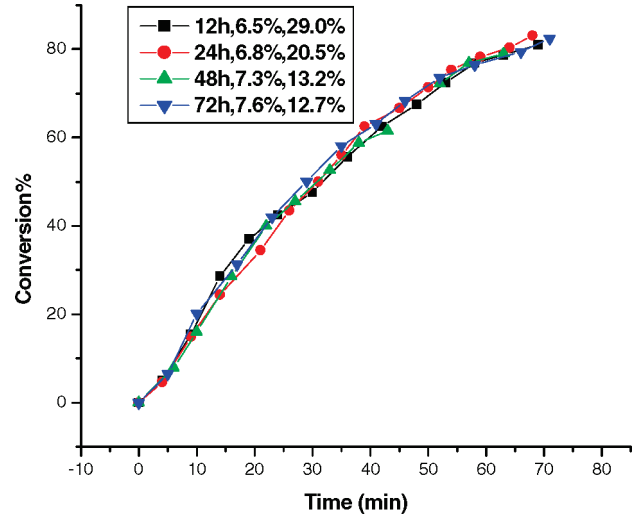


**Figure 4.** Plots of monomer conversion versus reaction time to compare the activities of Amberzyme−CALB catalysts that differ in the fractions of physically vs chemically immobilized CALB by variation of the immobilization time.

the polymerization rate. This further supports the assertion above that covalent immobilization of CALB through reaction with surface epoxy groups is a mild method that retains to a large extent CALB activity.

Variation in Amberzyme−CALB loading was achieved by using 100, 200, 300, and 400 mg CALB per g of resin, respectively, for 48 h incubation times. Polymerizations of ϵ-CL were performed using Amberzyme−CALB with enzyme loadings of 4.0% (0.18 $mg/m^2$), 7.6% (0.36 $mg/m^2$), 10.5% (0.52 $mg/m^2$), and 12.3% (0.61 $mg/m^2$). Catalyst quantities were adjusted so that all polymerizations with these resins were performed with 1:100 w/w CALB to ϵ-CL. Figure 5 shows small increases in catalyst activity with increased CALB loading. For example, at ~20 min reaction time, as enzyme loading increased from 4.0 to 7.6, 10.5, and 12.3%, ϵ-CL % conversion increased from 17 to 18, 21, and 23%, respectively. Correspondingly, TOF increased from 4.1 to 4.4, 4.9, and 5.5 $s^{-1}$. Also, reaction kinetic constants ($k_{app}$) from slopes of $\log([M_o]/[M])$ versus time plots (Figure 5B) increased from 0.0020 to 0.0025, 0.0030, and 0.0033, respectively. This increase in activity with higher CALB loading is reflected in changes in active site availability determined by active site titration with MNPHP (see Experimental Section). Table 1 shows the fraction of active CALB molecules increased from 13.6 to 15.5, 19.4, 22.7, and 25.0% with increase in enzyme loading from 1.9 to 4.0, 7.6, 10.5, and 12.3%, respectively. Indeed, other studies showed enzyme loading is an important adjustable parameter for catalyst optimization. For example, Kondon et al.[45] obtained similar trends when determining relationships between trypsin, peroxidase, and catalase loading onto Ultrafine silica particles and enzyme activity. Lee and Belfort,[46] by measuring adsorbed layer thickness, suggested that with increased loading, protein–protein interaction prevented conformation change/unfolding by reorganizing protein molecules from side-on to end-on binding. This change in binding mode resulted in greater exposure of enzyme active sites to substrates, thereby leading to increased enzyme activity. Relative to this study, larger increases in CALB activity was achieved by adjusting CALB loading by physical adsorption onto a PMMA resin (35 μm diameter, 250 Å pore size).[5] Specifically, during 30 min reactions using the PMMA−CALB catalyst, as CALB loading increased from 2.6 to 4.3 and 5.7%, ϵ-CL TOF increased from 1.0 to 5.2 and 11.2 $s^{-1}$, respectively.

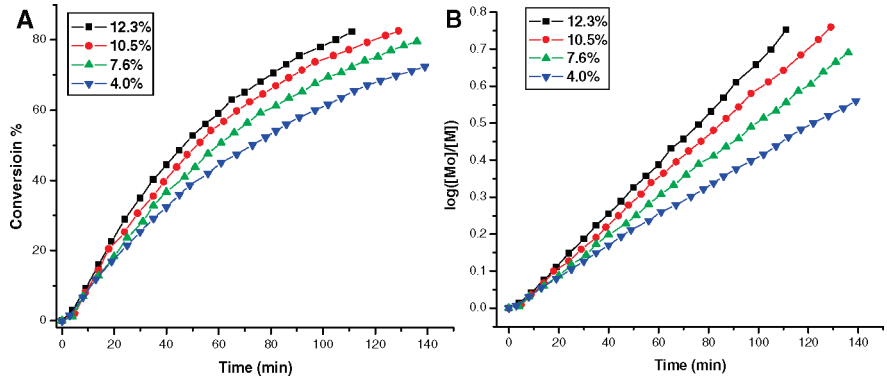


**Figure 5.** Effect of CALB loading on the catalytic activity of Amberzyme−CALB catalysts. Activities were measured by performing $\epsilon$-caprolactone ring-opening polymerizations at 70 °C in toluene. (A) and (B) display plots of % monomer conversion vs time and semilogarithmic plots, respectively.

**Table 1.** Enzyme Loading, Active Site Titration, and Reaction Constant ($k_{app}$) Values for Amberzyme−CALB Catalysts

| concentration of CALB (mg/mL) | enzyme loading (%) | reaction constant[a] | active sites (%) |
|---|---|---|---|
| 0.5 | 1.9 | nd[b] | 13.6 ± 2.8 |
| 1 | 4.0 | 0.0020 | 15.5 ± 2.3 |
| 2 | 7.6 | 0.0025 | 19.4 ± 3 |
| 3 | 10.5 | 0.0030 | 22.7 ± 3.5 |
| 4 | 12.3 | 0.0033 | 25.0 ± 3.2 |

[a] Reaction constant values were determined by carrying out $\epsilon$-CL ring-opening polymerizations in toluene-$d_8$ at 70 °C for 70 min. [b] Not determined (nd). The reaction constant was not determined for Amberzyme−CALB with an enzyme loading of 1.9% due to weak NMR signal intensities.

This nonlinear relationship between enzyme concentration and reaction rate was partially explained by a larger fraction of active sites with increased CALB loading.[5] Furthermore, increase in enzyme loading can result in a more uniform distribution of enzyme throughout the beads, which was previously shown to be beneficial to catalyst activity.[35]

**Effects of Multiple Reaction Cycles on Polymerization Activity of Amberzyme−CALB and Novozyme 435.** A desired outcome of CALB immobilization by covalent bond formation instead of by physical adsorption is decreased leaching of CALB into product. By decreasing leakage of catalyst during a reaction, both product purity and catalyst recycling would be improved. To evaluate the potential of recycling Amberzyme−CALB, $\epsilon$-CL ring-opening polymerization was performed in toluene at 70 °C for 70 min, the catalyst was recovered by removal of solvent, beads were washed three times with THF and once with toluene-$d_8$, and then the above steps were repeated for two additional reaction cycles (see Experimental Section for additional details). Inspection of Figure 6 shows that, over three reaction cycles, % $\epsilon$-CL versus time plots appear identical. These results suggest that, over three reaction cycles under the above reaction conditions, no significant leaching of CALB from Amberzyme−CALB or denaturation of immobilized CALB occurred. In comparison, physi-adsorbed CALB on Lewatit VPOC 1600 (i.e., Novozym 435) was used as catalyst for three $\epsilon$-CL ring-opening polymerization cycles as above, and the results of this study are also shown in Figure 6. In contrast to Amberzyme−CALB, % $\epsilon$-CL versus time plots for Novozym 435 catalyzed polymerizations showed that 6 and 9% of catalyst activity was lost during the second and third cycles, respectively. This is likely due to some extent of CALB leakage from Novozym 435 during each reaction cycle.

To further assess Amberzym−CALB (7.6% by wt CALB) recyclability, studies were performed for polycondensation reactions. Amberzyme−CALB catalyzed bulk polycondensation

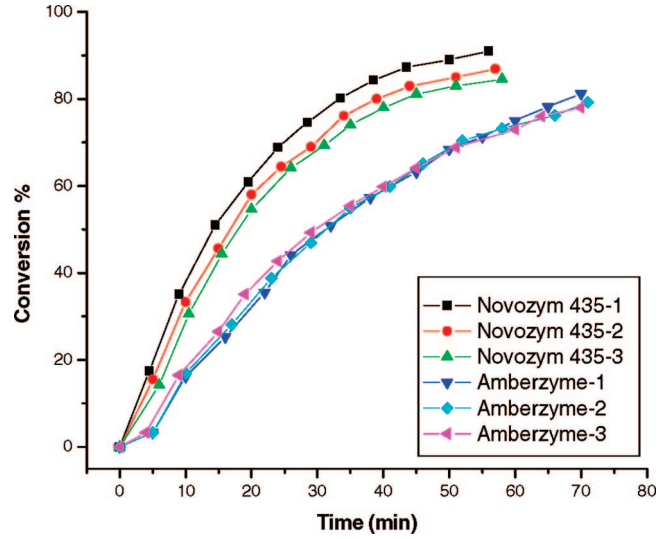


**Figure 6.** Amberzyme−CALB and Novozym 435 catalyzed $\epsilon$-CL ring-opening polymerizations in toluene-$d_8$ at 70 °C for 70 min. Reactions were conducted for three reaction cycles where the catalyst was recovered and reused.

reactions between glycerol (0.1 equiv), 1, 8-octanediol (0.4 equiv), and adipic acid (0.5 equiv) were carried out at 90 °C for 64 h. THF was added to the reaction. The catalyst was recovered by filtration, washed three times with THF, and then was reused for two additional reaction cycles (see Experimental Section). Inspection of Figure 7A shows that, over three reaction cycles, little change was observed in $M_n$ values although $M_w/M_n$ values increased from 1.8 to 2.3 and 2.8 for cycles 1, 2, and 3, respectively. At present, we do not understand what changes in Amberzym−CALB occurred over each reaction cycle that would cause a change in product polydispersity. For comparison, physi-adsorbed CALB on Lewatit VPOC 1600 (i.e., Novozym 435) was used as catalyst for three glycerol, 1,8-octanediol, and adipic acid polycondensation reaction cycles as above, and the results of this study are also shown in Figure 7B. The reaction was stopped after 24 h to achieve similar $M_w$. In contrast to Amberzyme−CALB, Novozym 435 catalyzed polycondensations over three reaction cycles showed large decreases in $M_w$ values during successive reaction cycles. Indeed, $M_w$ decreased from 32 400 using the native catalyst to 7500 and 1200 by using first and second time recovered Novozym 435, respectively. We believe that decreased activity of Novozym 435 over three reaction cycles is largely due to leakage of CALB. Determination of enzyme leaching into product as a function of enzyme immobilization method and

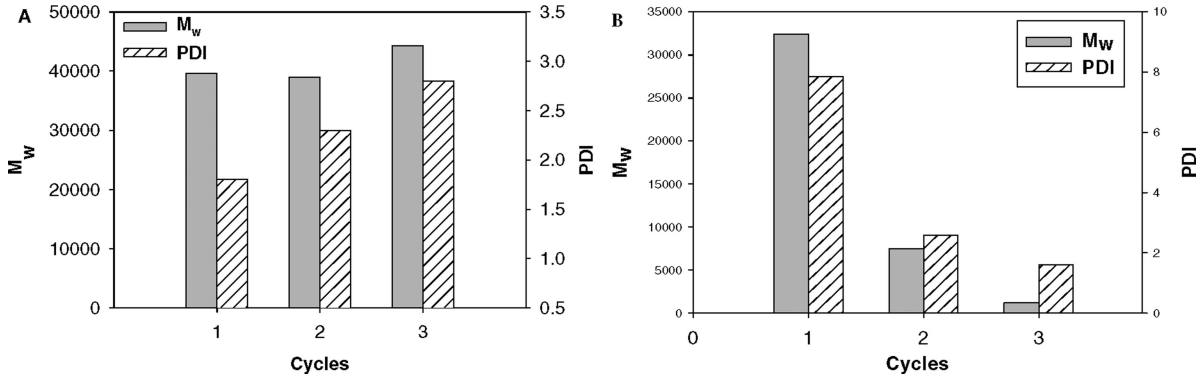


**Figure 7.** Amberzyme−CALB (A) and Novozym 435 (B) catalyzed bulk polycondensation reactions between glycerol (0.1 equiv), 1,8-octanediol (0.4 equiv), and adipic acid (0.5 equiv) performed at 90 °C for 64 and 24 h, respectively. Reactions were conducted for three reaction cycles where the catalyst was recovered and reused.

reaction conditions is currently under study and will be reported in a separate publication.

## Summary of Results

This work explored covalent immobilization of CALB on epoxy-activated carriers. Epoxy-activated Amberzyme macroporous beads were used that have average values of particle size, surface area, and pore diameter of 235 $\mu$m, 230 $m^2/g$, and 220 Å, respectively. For comparison, epoxy-activated nanoparticles (nanoPSG, 68 nm) were prepared and used to immobilize CALB. IR microspectroscopy of Amberzyme−CALB (7.3% CALB loading) revealed CALB is localized within a loading front of 50 $\mu$m thickness. This result is consistent with a previous report by our laboratory on Novozym 435. Formation of a loading front for both of these catalysts is believed to be a consequence of CALB's strong affinity for bead surfaces and low affinity or repulsive interactions between immobilized and soluble CALB molecules. The result is limited diffusion and subsequent immobilization of soluble CALB at internal bead regions. To probe the extent to which CALB is chemically immobilized on epoxy-activated Amberzyme beads, Amberzyme−CALB was extracted with DMSO and Triton X-100 solutions. For CALB loading of about 7%, the majority of CALB molecules on Amberzyme−CALB are covalently linked by a 12 h incubation time.

Large differences were found in activity for the three immobilized CALB catalysts studied herein. Specifically, at about 20 min reaction time, the turnover frequency (TOF) for $\epsilon$-CL increased from 4.4 to 10.5 and 39.2 $s^{-1}$ for Amberzym−CALB, Novozym 435, and nanoPSG−CALB, respectively. The high activity of nanoPSG relative to the other catalysts was largely attributed to its small size and nonporosity that circumvents diffusion constraints encountered for Lewatit VPOC 1600 and Amberzyme−CALB. The higher activity of Novozym 435 relative to Amberzyme−CALB for $\epsilon$-CL ring-opening is largely due to differences in active-site availability. Work is currently in progress to adjust Amberzyme surface chemistry to alter CALB orientation upon binding so that the fraction of CALB free active sites is increased.

By using Amberzyme−CALB as catalyst for $\epsilon$-CL ring-opening polymerizations (70 °C, 70 min) over three reaction cycles, % $\epsilon$-CL versus time plots appear identical. Similarly, Amberzyme−CALB catalyzed bulk polycondensation reactions between glycerol (0.1 equiv), 1,8-octanediol (0.4 equiv), and adipic acid (0.5 equiv), performed for three reaction cycles (each at 90 °C for 24 h) showed similar product $M_w$ values. Further comparative recycling studies using Novozym 435 led to the conclusion that covalent immobilization of CALB on Amberzyme as opposed to physical immobilization of CALB on Lewatit VPOC 1600 (e.g., Novozym 435) gave superior recyclability. This work provides an important foundation for the development of CALB catalysts prepared by immobilization on supports via epoxy-activated moieties. The resulting chemically immobilized catalysts show promising catalytic properties for polyester synthesis.

**Acknowledgement.** . We thank the NSF and Industrial members (BASF, Novozymes, Johnson & Johnson, Rohm and Haas, Genencor, Estée Lauder, DNA 2.0, W. R. Grace, Grain Processing Corporation, and DeGussa) of the NSF-Industry/University Cooperative Research Center (NSF-I/UCRC) for Biocatalysis and Bioprocessing of Macromolecules at Polytechnic University for their financial support, intellectual input, and encouragement during the course of this research. We are also grateful to Dr. Lisa Miller and colleagues for providing access to the FTIR facilities at the National Synchrotron Light Source (Brookhaven National Laboratory, Upton, New York 11973).

## References and Notes

(1) Kirk, O.; Christensen, M. W. *Org. Process Res. Dev.* **2002**, *6*, 446–451.
(2) Anderson, E. M.; Larsson, K. M.; Kirk, O. *Biocatal. Biotransform.* **1998**, *16*, 181–204.
(3) Kirk, O.; Björkling, F.; Godtfredsen, S. E.; Larsen, T. O. *Biocatalysis* **1992**, *6*, 127–134.
(4) Mateo, C.; Palomo, J. M.; Fernandez-Lorente, G.; Guisan, J. M.; Fernandez-Lafuente, R. *Enzyme Microb. Technol.* **2007**, *40*, 1451–1463.
(5) Chen, B.; Miller, E. M.; Miller, L.; Maikner, J. J.; Gross, R. A. *Langmuir* **2007**, *23*, 1381–1387.
(6) Singh, S. K.; Felse, A. P.; Nunez, A.; Foglia, T. A.; Gross, R. A. *J. Org. Chem* **2003**, *68*, 5466–5477.
(7) Weber, N.; Weitkamp, P.; Mukherjee, K. D. *J. Agric. Food Chem.* **2001**, *49*, 5210–5216.
(8) Hamam, F.; Shahidi, F. *J. Agric. Food Chem.* **2006**, *54*, 4390–4396.
(9) Maugard, T.; Tudella, J.; Legoy, M. D. *Biotechnol. Prog.* **2000**, *16*, 358–362.
(10) Jeon, N. Y.; Ko, S.-J.; Won, K.; Kang, H.-Y.; Kim, B. T.; Lee, Y. S.; Lee, H. *Tetrahedron Lett.* **2006**, *47*, 6517–6520.
(11) Gross, R. A.; Kalra, B. *Science* **2002**, *297*, 803–806.
(12) Gross, R. A.; Kumar, A.; Kalra, B. *Chem. Rev.* **2001**, *101*, 2097–2124.
(13) Kobayashi, S.; Uyama, H.; Kimura, S. *Chem. Rev.* **2001**, *101*, 3793.
(14) Bisht, K. S.; Deng, F.; Gross, R. A.; Kaplan, D. L.; Swift, G. *J. Am. Chem. Soc.* **1998**, *120*, 1363–1367.
(15) Persson, B. A.; Larsson, A. L. E.; Le Ray, M.; Backvall, J.-E. *J. Am. Chem. Soc.* **1999**, *121*, 1645–1650.

(16) Kumar, A.; Gross, R. A. *J. Am. Chem. Soc.* **2000**, *122*, 11767–11770.
(17) Mahapatro, A.; Kumar, A.; Kalra, B.; Gross, R. A. *Macromolecules* **2004**, *37*, 35–40.
(18) Palomo, J. M.; Fernandez-Lorente, G.; Mateo, C.; Manuel, F.; Fernandez-Lafuente, R.; Guisan, J. M. *Tetrahedron: Asymmetry* **2002**, *13*, 1337–1345.
(19) Lozano, P.; Perez-Marin, A. B.; De Diego, T.; Gomez, D.; Paolucci-Jeanjean, D.; Belleville, M. P.; Rios, G. M.; Iborra, J. L. *J. Membr. Sci* **2002**, *201*, 55–64.
(20) Fernandez-Lorente, G.; Palomo, J.; Mateo, C.; Munilla, R.; Ortiz, C.; Cabrera, Z.; Guisan, J. M.; Fernandez-Lafuente, R. *Biomacromolecules* **2006**, *7*, 2610–2615.
(21) Mahmoudian, M.; Rudd, B. A. M.; Cox, B.; Drake, C. S.; Hall, R. M.; Stead, P.; Dawson, M. J.; Chandler, M.; Livermore, D. G.; Turner, N. J.; Jenkins, G. *Tetrahedron* **1998**, *54*, 8171.
(22) Carrea, G.; Corcelli, A.; Palmisano, G.; Riva, S. *Biotechnol. Bioeng.* **1996**, *52*, 648.
(23) Brocklebank, S.; Woodley, J. M.; Lilly, M. D. *J. Mol. Catal. B: Enzym.* **1999**, *7*, 223.
(24) Ordaz, E.; Garrido-Pertierra, A.; Gallego, M.; Puyet, A. *Biotechnol. Prog.* **2000**, *16*, 287.
(25) Mateo, C.; Abian, O.; Fernandez-Lafuente, R.; Guisan, J. M. *Enzyme Microb. Technol.* **2000**, *26*, 509–515.
(26) Huwig, A.; Danneel, H.-J.; Giffhorn, F. *J. Biotechnol.* **1994**, *32*, 309.
(27) Ivanov, A. E.; Schneider, M. P. *J. Mol. Catal. B: Enzym.* **1997**, *3*, 303–309.
(28) Mateo, C.; Abian, O.; Fernandez-Lafuente, R.; Guisan, J. M. *Enzyme Microb. Technol.* **2000**, *26*, 509.
(29) Bosley, J. A.; Clayton, J. C. *Biotechnol. Bioeng.* **1994**, *43*, 934–938.
(30) Darkow, R.; Groth, Th.; Albrecht, W.; LuK tzow, K.; Paul, D. *Biomaterials* **1999**, *20*, 1277–1283.
(31) Wilkinson, M. C.; Hearn, J.; Cope, P.; Chainey, M. A. *Brit. Polym. J.* **1981**, *13*, 82–91.
(32) (a) Mateo, C.; Fernandez-Lorente, G.; Abian, O.; Fernandez-Lafuente, R.; Guisan, J. M. *Biomacromolecules* **2000**, *1*, 739. (b) Wheatley, J. B.; Schmidt, D. E. *J. Chromatogr.* **1993**, *644*, 11–16. (c) Wheatley, J. B.; Schmidt, D. E. *J. Chromatogr.* **1999**, *849*, 1–12.
(33) Dennis, K. E.; Clark, D. S.; Bailey, J. E.; Cho, Y. K.; Park, Y. H. *Biotechnol. Bioeng.* **1984**, *26*, 892–900.
(34) Uppenberg, J.; Hansen, M. T.; Patkar, S.; Jones, T. A. *Structure* **1994**, *2*, 293–308.
(35) Mei, Y.; Miller, L.; Gao, W.; Gross, R. A. *Biomacromolecules* **2003**, *4*, 70–74.
(36) Malmsten, M.; Larsson, A. *Colloids Surf., B* **2000**, *18*, 277–284.
(37) Deng, F.; Gross, R. A. *Int. J. Biol. Macromol.* **1999**, *25*, 153–159.
(38) Henderson, L. A.; Svirkin, Y. Y.; Gross, R. A.; Kaplan, D. L.; Swift, G. *Macromolecules* **1996**, *29*, 7759–7766.
(39) Mei, Y.; Kumar, A.; Gross, R. *Macromolecules* **2003**, *36*, 5530–5536.
(40) Vertegel, A. A.; Siegel, R. W.; Dordick, J. S. *Langmuir* **2004**, *20*, 6800–6807.
(41) (a) Torii, H.; Tasumi, M. *Infrared Spectroscopy of Biomolecules*; Mantsch, H. H., Chapman, D., Eds.; John Wiley & Sons: New York, 1996, pp 1–18. (b) Krimm, S.; Bandekar, J. *Adv. Protein Chem.* **1986**, *38*, 181. (c) Susi, H.; Byler, D. M. *Methods Enzymol.* **1986**, *130*, 290. (d) Pancoska, P.; Wang, L.; Keiderling, T. A. *Protein Sci.* **1993**, *2*, 411.
(42) Susi, H.; Byler, D. M. *Biochem. Biophys. Res. Commun.* **1983**, *115*, 391–397.
(43) Nakaoki, T.; Mei, Y.; Miller, L. M.; Kumar, A.; Kalra, B.; Miller, M. E.; Kirk, O.; Christensen, M.; Gross, R. A. *Ind. Biotechnol.* **2005**, *1*, 126–134.
(44) Chen, B.; Miller, M. E.; Gross, R. A. *Langmuir* **2007**, *23*, 6467–6474.
(45) Kondo, A.; Murakami, F.; Kawagoe, M.; Higashitani, K. *Appl. Microb. Technol.* **1993**, *39*, 726.
(46) Lee, C. S.; Belfort, G. *Proc. Natl. Acad. Sci. U.S.A.* **1989**, *86*, 8392–8396.

BM700949X